scientific reports

Check for updates

OPEN

Identification of immune-related genes as prognostic factors in bladder cancer

Jie Zhu[1,9], Han Wang[2,9], Ting Ma[1,9], Yan He[3], Meng Shen[4], Wei Song[5], Jing-Jing Wang[6], Jian-Ping Shi[3], Meng-Yao Wu[4], Chao Liu[7], Wen-Jie Wang[3]✉ & Yue-Qing Huang[8]

Bladder cancer is one of the most common cancers worldwide. The immune response and immune cell infiltration play crucial roles in tumour progression. Immunotherapy has delivered breakthrough achievements in the past decade in bladder cancer. Differentially expressed genes and immune-related genes (DEIRGs) were identified by using the edgeR package. Gene ontology annotation and Kyoto Encyclopedia of Genes and Genomes (KEGG) pathway analyses were performed for functional enrichment analysis of DEIRGs. Survival-associated IRGs were identified by univariate Cox regression analysis. A prognostic model was established by univariate COX regression analysis, and verified by a validation prognostic model based on the GEO database. Patients were divided into high-risk and low-risk groups based on the median risk score value for immune cell infiltration and clinicopathological analyses. A regulatory network of survival-associated IRGs and potential transcription factors was constructed to investigate the potential regulatory mechanisms of survival-associated IRGs. Nomogram and ROC curve to verify the accuracy of the model. Quantitative real-time PCR was performed to validate the expression of relevant key genes in the prognostic model. A total of 259 differentially expressed IRGs were identified in the present study. KEGG pathway analysis of IRGs showed that the "cytokine-cytokine receptor interaction" pathway was the most significantly enriched pathway. Thirteen survival-associated IRGs were selected to establish a prognostic index for bladder cancer. In both TCGA prognostic model and GEO validation model, patients with high riskscore had worse prognosis compared to low riskscore group. A high infiltration level of macrophages was observed in high-risk patients. OGN, ELN, ANXA6, ILK and TGFB3 were identified as hub survival-associated IRGs in the network. EBF1, WWTR1, GATA6, MYH11, and MEF2C were involved in the transcriptional regulation of these survival-associated hub IRGs. The present study identified several survival-associated IRGs of clinical significance and established a prognostic index for bladder cancer outcome evaluation for the first time.

With an estimated 81,190 newly diagnosed cases and 17,240 deaths occurring in 2018, bladder cancer (BC) ranks as the fifth most common cancer in the USA[1]. Multiple risk factors are involved in the occurrence and development of bladder cancer, among which tobacco smoke is a principal risk factor[2]. Previous studies have reported that approximately 70% of BCs are at a non-muscle-invasive stage at diagnosis, and bladder resection is the standard treatment for these patients[3]. For metastatic or unresectable bladder cancer, platinum-based chemotherapy has been certified as the standard first-line treatment[4]. However, traditional chemotherapy has shown no effect on prolonging overall survival (OS)[5].

[1]Department of Oncology, Changzhou Traditional Chinese Medical Hospital, Changzhou 213003, Jiangsu, People's Republic of China. [2]Department of Oncology, Jining Tumour Hospital, Jining, People's Republic of China. [3]Department of Radio-Oncology, The Affiliated Suzhou Hospital of Nanjing Medical University, Suzhou 215001, Jiangsu, People's Republic of China. [4]Department of Oncology, The First Affiliated Hospital of Soochow University, Suzhou 215006, Jiangsu, People's Republic of China. [5]Department of Gastrointestinal Surgery II, Renmin Hospital of Wuhan University, Wuhan, People's Republic of China. [6]Department of Oncology, Taizhou Hospital of Traditional Chinese Medicine, Taizhou, People's Republic of China. [7]Department of Urology, The Affiliated Suzhou Hospital of Nanjing Medical University, Suzhou 215001, Jiangsu, People's Republic of China. [8]Department of General Practice, The Affiliated Suzhou Hospital of Nanjing Medical University, Suzhou, People's Republic of China. [9]These authors contributed equally: Jie Zhu, Han Wang and Ting Ma. ✉email: doctor.wjwang@gmail.com

The correlation between clinical outcomes and the density of tumour immune infiltration has been confirmed in previous studies[6]. Strong evidence demonstrates that innate immune cells, including lymphocytes, macrophages, neutrophils and dendritic cells, play a crucial role in cancer development[7]. With complex interactions with tumour cells in the tumour microenvironment, these immune cells not only fail to work against tumour cells but also mediate immune tolerance and act as tumour promoters[8].Immunotherapy has delivered breakthrough achievements in several cancer types in the past decade[9–12]. Outstandingly, recent studies and clinical trials have made encouraging progress in immunotherapy for metastatic bladder cancer since the U.S. The Food and Drug Administration (FDA) approved the application of immune checkpoint agents in bladder cancer treatment. For instance, MPDL3280A (anti-PD-L1) has been demonstrated to show remarkable activity in metastatic bladder cancer[9].

While immunotherapy has improved the outcome of bladder cancer, the immunogenomic landscape of bladder cancer still remains unknown. In the present study, we aimed to investigate the impact of immune-related genes (IRGs) on prognosis prediction and identify potential prognostic biomarkers for bladder cancer.

Result

Identification of differentially expressed genes (DEGs) and differentially expressed IRGs (DEIRGs). The edgeR package in the R language was used to further analyse the data. To identify differentially expressed genes, a |log2 fold change (FC)|> 1.5 and a false discovery rate (FDR) adjusted to a $p < 0.01$ were set as the thresholds. Additionally, heat maps and volcano maps of the differentially expressed RNAs were generated by using the gplots and heatmap packages in the R platform. Among the 4880 differentially expressed genes, 3458 up-regulated genes and 1422 down-regulated genes were identified (Fig. 1A,B). Among the set of differentially expressed genes, 259 differentially expressed IRGs (DEIRGs) were screened out, including 140 up-regulated and 119 down-regulated genes (Fig. 1C,D). In Gene Ontology (GO) analysis of DEGs, a total of 10 significantly enriched pathways were obtained (Supplementary material 1). The results indicated that the extracellular region was the most frequent GO biological process category ($p < 0.05$) (Supplementary material 2). In the KEGG pathway analysis, a total of 10 significantly enriched pathways were obtained. Among the top 10 pathways, "MAPK signalling pathway", "IL-17 signalling pathway", "cytokine-cytokine interaction receptor", "neuroactive ligand-receptor interaction" and "viral protein interaction with cytokine and cytokine receptor" were identified as the top 5 enriched pathways. A visual network between IRGs and the top 5 KEGG pathways was constructed by using Cytoscape v3.6.1 (Supplementary material 3). Cytokine-cytokine receptor interaction was the most frequent KEGG pathway category ($p < 0.05$) (Supplementary material 4). In GO analysis of DEIRGs, the extracellular region was the most frequent GO biological process category ($p < 0.05$) (Supplementary material 5). In the KEGG pathway analysis, the MAPK signalling pathway was the most frequent KEGG pathway category ($p < 0.05$) (Supplementary material 6).

Identification of differentially expressed transcription factors. To investigate the regulatory mechanisms of these IRGs, we further examined the expression profiles of 77 transcription factors (TFs). Among the 77 differentially expressed TFs, 34 up-regulated TFs and 41 down-regulated TFs were identified (Fig. 2).

Evaluation of clinical outcomes. Based on univariate Cox regression analysis, we identified 27 survival-associated IRGs, constructed a prognostic index containing 13 survival-associated IRGs by multiple Cox regression analysis (Fig. 3), and separated BC patients into two groups (high risk score group and low risk score group) with regard to OS and median risk score (Fig. 4A–C). The prognostic model was verified by a validation prognostic model based on the GEO database. In the validation model (Fig. 4D–F).The survival risk score was calculated as follows:

$$Survival\ Risk\ Score(SRS) = \sum_{i=1}^{k} (C_i \times V_i)$$

The formula was as follows: [expression level of ADIPOQ* 0.081574] + [expression level of AHNAK* 0.012963] + [expression level of CALR* 0.001428] + [expression level of CMTM8* 0.035383] + [expression level of EDNRA* 0.084329] + [expression level of MMP9* 0.001393] + [expression level of NAMPT* 0.022201] + [expression level of PPY* 0.455283] + [expression level of PROK1* 0.149154] + [expression level of RAC3* 0.024755] + [expression level of RBP7* 0.015126] + [expression level of SLIT2* − 0.31961] + [expression level of STAT1* − 0.0065]. We classified patients into high and low risk score groups based on the median riskscore as the cut-off, the survival was analyzed by KM curve. In TCGA prognostic model, high risk score group had worse OS compared to the low riskscore group, $p < 0.001$ (Fig. 5A). In the validation model, high risk score group had worse OS compared to the low riskscore group, $p < 0.001$ (Fig. 5B).

Clinical application of the prognostic index. The relationship between the prognostic index and clinicopathological features was analysed, including age, sex, American Joint Committee on Cancer (AJCC) stage, tumour stage and lymph node metastasis. Univariate analyses demonstrated that older age (hazard ratio [HR]2.003; 95% CI 1.547–2.592; $p < 0.001$), advanced AJCC stage (HR1.039; 95% CI 1.019–1.059; $p < 0.001$), high T stage (HR 1.629; 95% CI 1.240–2.141; $p < 0.001$), high N stage (HR 1.566; 95% CI 1.302–1.883; $p < 0.001$) and high risk score (HR 1.039; 95% CI 1.027–1.051; $p < 0.001$) were significant risk factors for poor outcome (Fig. 5C). Multivariate analysis indicated that a high risk score (HR 1.809; 95% CI 1.100–2.977; $p < 0.001$) and

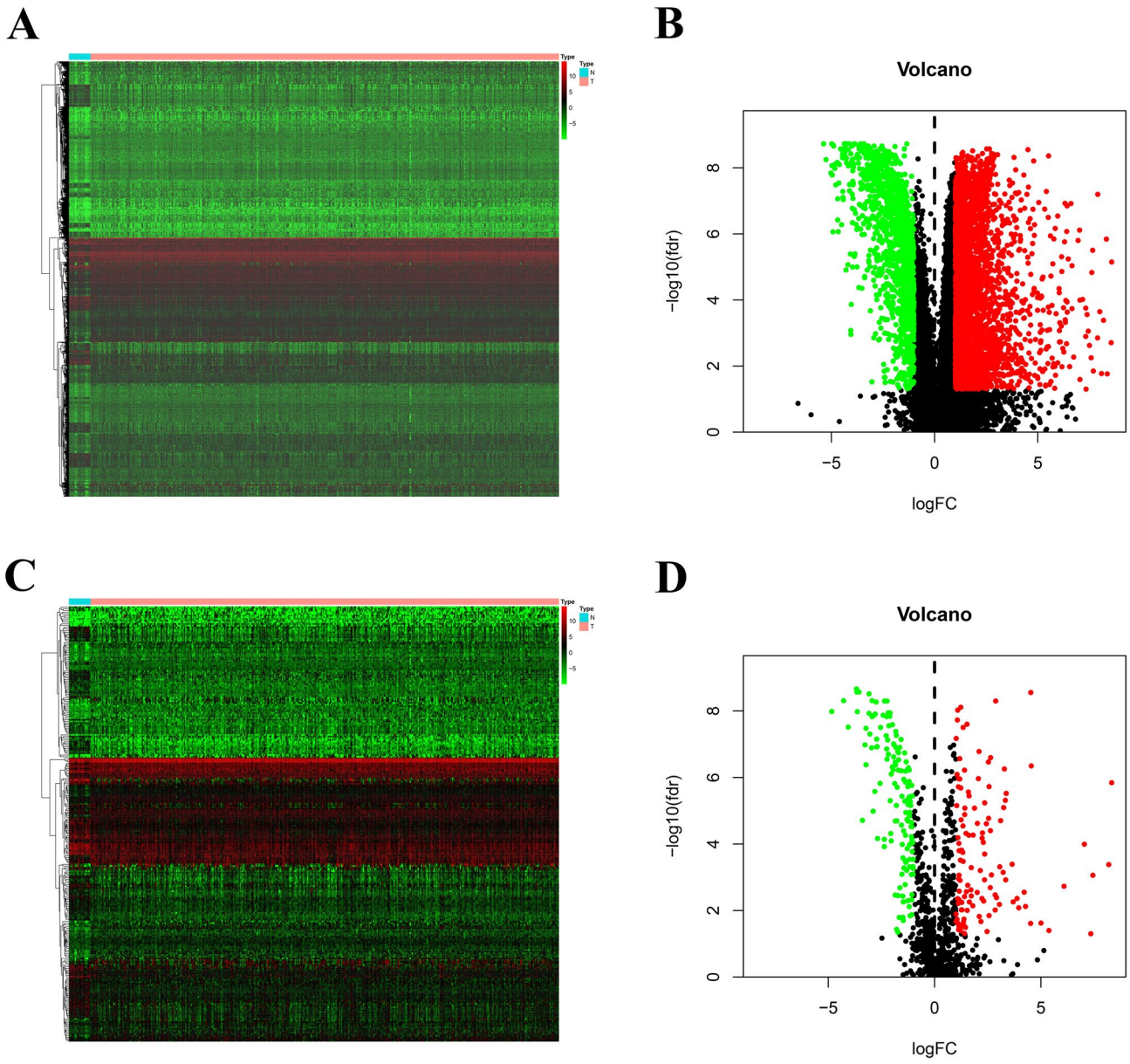

Figure 1. Differentially expressed genes (DEGs) and immune-related genes (DEIRGs): The heatmap (**A**) and volcano (**B**) of DEGs between bladder cancer tissues and no-cancer tissues. The heatmap (**C**) and volcano (**D**) of DEIRGs between bladder cancer tissues and no-cancer tissues.

high T stage (HR 1.530; 95% CI 1.045–2.239; $p < 0.001$) were independently associated with worse OS (Fig. 5D). Of interest, for individual IRGs, our data also showed a close correlation with clinicopathological features (Supplementary material 7–9. In validation prognostic model, univariate analyses showed that older age (HR = 1.032; 95% CI = 1.012–1.052; $p < 0.001$) and high risk score (HR = 2.357; 95% CI = 1.748–4.277; $p < 0.001$) were significant risk factors for poor prognosis (Fig. 5E). Multivariate analysis indicated that a high risk score (HR 1.920; 95% CI 1.162–3.172; $p = 0.011$) and high T stage (HR 1.688; 95% CI 1.122–2.480; $p = 0.011$) were found to be independently associated with worse OS (Fig. 5F).

Verify the accuracy of the prognostic model. In order to further verify the accuracy of the prognostic model, we constructed the diagram and ROC curve respectively. The ROC curve analysis of TCGA prognostic model was showed in Fig. 6A. The TCGA prognostic model of nomogram was showed in Fig. 6C, and the C-index was 0.734. The ROC curve analysis of GSE31684 validated prognostic model was showed in Fig. 6B. The GSE31684 validated prognostic model of nomogram was showed in Fig. 6D, and the C-index was 0.711.

Prognostic index and immune cell infiltration correlation analysis. Among six immune cell subtypes, including B cells, CD4 cells, CD8 cells, dendritic cells, macrophages and neutrophils, a high infiltration level of macrophages was observed in high-risk patients (Cor = 0.241, $p < 0.001$) (Fig. 7).

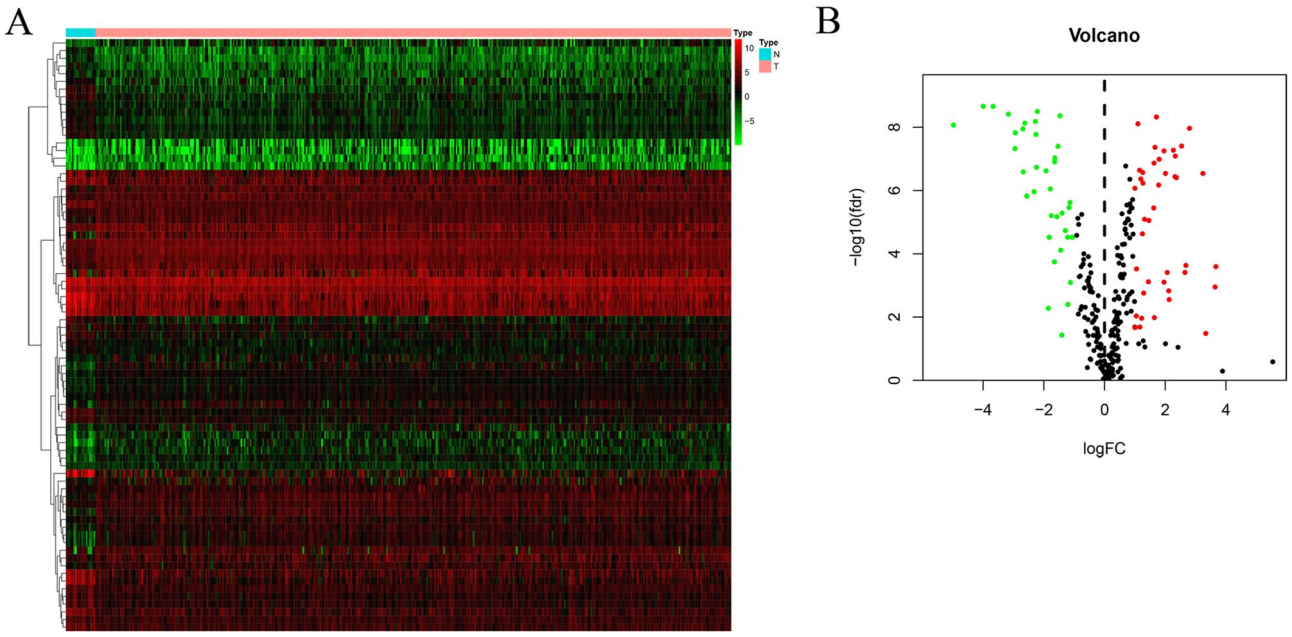

Figure 2. Differentially expressed transcription factors (DETFs): the heatmap (**A**) and volcano (**B**) of DETFs between bladder cancer tissues and no-cancer tissue.

Regulatory mechanisms of survival-associated IRGs. OGN, ELN, ANXA6, ILK and TGFB3 were identified as hub survival-associated IRGs in the network. EBF1, WWTR1, GATA6, MYH11, and MEF2C were involved in the transcriptional regulation of these survival-associated hub IRGs (Supplementary material 10).

Analysis and validation of gene expression. To further validate the expression of relevant key genes in the prognostic model, we randomly selected 6 genes to measure the expression level in BC tissue and adjacent normal tissues. We found that the expression is consistent with the TCGA database and GSE31684 (Fig. 8).

Discussion

The host immune system is well acknowledged to play a pivotal role in tumour initiation and development[13]. Immune cells, an important component of the tumour microenvironment, have shown promise as clinical biomarkers for a variety of malignant tumours[7,8,14]. Previous studies have conducted in-depth investigations of immune-related genes (IRGs) in several cancer types, including gastric cancer[15,16], pancreatic cancer[17], thyroid cancer[18], and non-small-cell lung cancer[19]. However, few studies have explored the role of IRGs in and their predictive value for clinical outcomes in bladder cancer. In the present study, we aimed to construct an immunogenomic prognostic signature based on survival-related IRGs and investigate prognostic biomarkers and potential clinical targeted therapies in bladder cancer.

In the present study, we identified 54 differentially expressed survival-associated IRGs. RAC, a type of Rho-GTPase, is composed of three proteins named RAC1, RAC2, and RAC3[20]. RAC3 has been proven to participate in cell migration, adhesion and apoptosis, playing an important role in breast cancer and lung adenocarcinoma[21–25]. In the study of Walker et al.[22] RAC3 promoted cancer cell migration, and overexpression of RAC3 in ER-positive breast cancer was correlated with decreased recurrence-free survival. In a recent study, RAC3 was identified to be correlated with the prognosis of prostate cancer[26]. Endothelin A receptor (EDNRA), a G-protein-coupled receptor for endothelin, is widely expressed on vascular smooth muscle cells[27]. ENDRA was strongly correlated with worse outcomes in ovarian cancer[28]. Additionally, Laurberg et al.[29] reported that high expression of ENDRA was correlated with decreased cancer-specific survival and poor outcome in patients with advanced bladder cancer. AHNAK, a type of desmoyokin, has been shown to be involved in a series of cellular processes, including malignant migration and invasion[30]. Opinions vary regarding the role of AHNAK in tumour progression and outcome prediction. In a recent study by Chen et al.[31] AHNAK was demonstrated to suppress tumour proliferation and invasion in triple-negative breast cancer. Moreover, AHNAK acts as a tumour suppressor, and down-regulation of AHNAK was independently associated with poor outcome in glioma[32]. Nevertheless, up-regulation of AHNAK was correlated with poor outcome in pancreatic cancer[33].

In the KEGG pathway analysis, "MAPK signalling pathway", "IL-17 signalling pathway", "cytokine-cytokine interaction receptor", "neuroactive ligand-receptor interaction" and "viral protein interaction with cytokine and cytokine receptor" were identified as the top 5 enriched pathways. Mitogen-activated protein kinases (MAPKs) participate in a series of biological functions, including cell proliferation, angiogenesis, and metastasis of malignant tumours, including bladder cancer[34–36]. For instance, in a recent study by Zhao et al.[36] benzidine was demonstrated to enhance the proliferation of bladder cells via the MAPK/AP-1 signalling pathway. To date, up-regulation of pyruvate kinase M2 has been shown to promote bladder cancer metastasis by facilitating cell

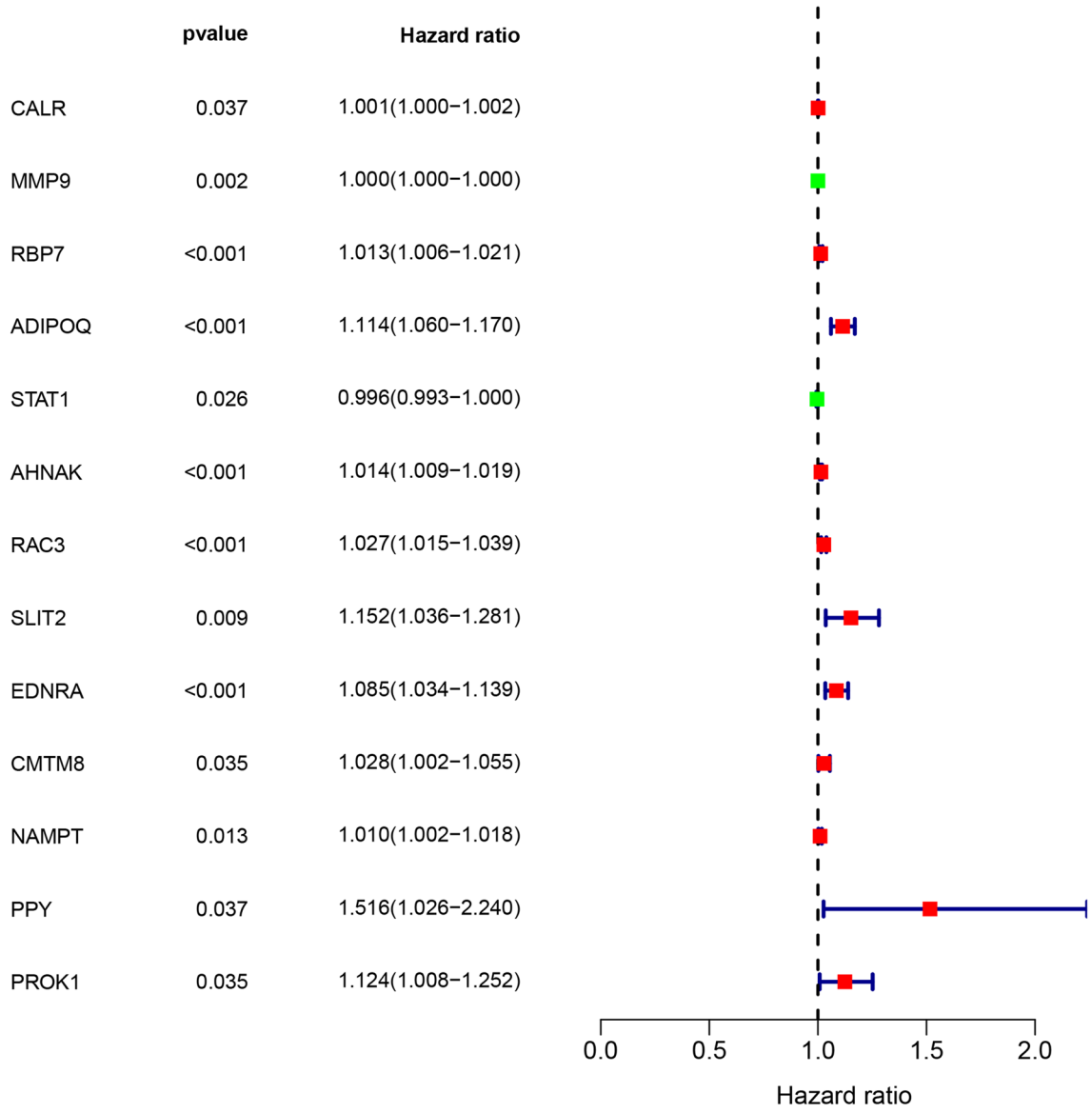

Figure 3. Prognostic values of survival-associated IRGs: the forest plot of survival-associated IRGs.

proliferation, invasion and migration via the MAPK signalling pathway[37]. Moreover, the present study indicated that RAC3 was affected by the MAPK signalling pathway. RAC3 has been demonstrated to promote cell invasion and migration via the p38 MAPK pathway in lung adenocarcinoma[25]. To the best of our knowledge, no studies have reported the correlation between RAC3 and the MAPK signalling pathway in bladder cancer. Thus, the molecular mechanism of MAPK signalling pathway regulation is worthy of exploration and study.

The present study constructed a prognostic index for bladder cancer for the first time. Our prognostic index showed promising clinical feasibility. Our findings indicated that patients with high risk scores showed more advanced stages and larger tumour sizes than patients with low risk scores. Of interest, for individual IRGs, our data also showed a close correlation with clinicopathological features. For instance, up-regulation of ADIPOQ, AGTR1, AHNAK, ENDRA, RBP7 and SLIT2 was correlated with larger tumour size and more advanced tumour stage. RLN2 and NAMPT were correlated with sex.

Moreover, a combinatory analysis of immune cell infiltration and prognostic index was performed to investigate the tumour immune microenvironment. In the present study, the prognostic index had a significantly positive correlation with the infiltration of macrophages. This result indicated that a higher infiltration level of macrophages was probably observed in high-risk patients. With the influence of chemoattractants and other stimuli, circulating monocytes are recruited into the tumour site and differentiate into tumour-associated macrophages (TAMs)[38]. TAMs can be categorized into the anti-tumour M1 phenotype and the pro-tumorigenic M2 phenotype, and the M2 phenotype accounts for the majority of TAMs[39]. Notably, M2-phenotype TAMs have been correlated with poor clinical outcomes in pancreatic cancer, breast cancer and lung cancer[40,41]. $CD204^{+}$ macrophages, in other words, M2 macrophages, were significantly associated with larger tumour size, more advanced tumour stage, higher tumour grade and more nodal metastasis in bladder cancer[42]. Coincidentally,

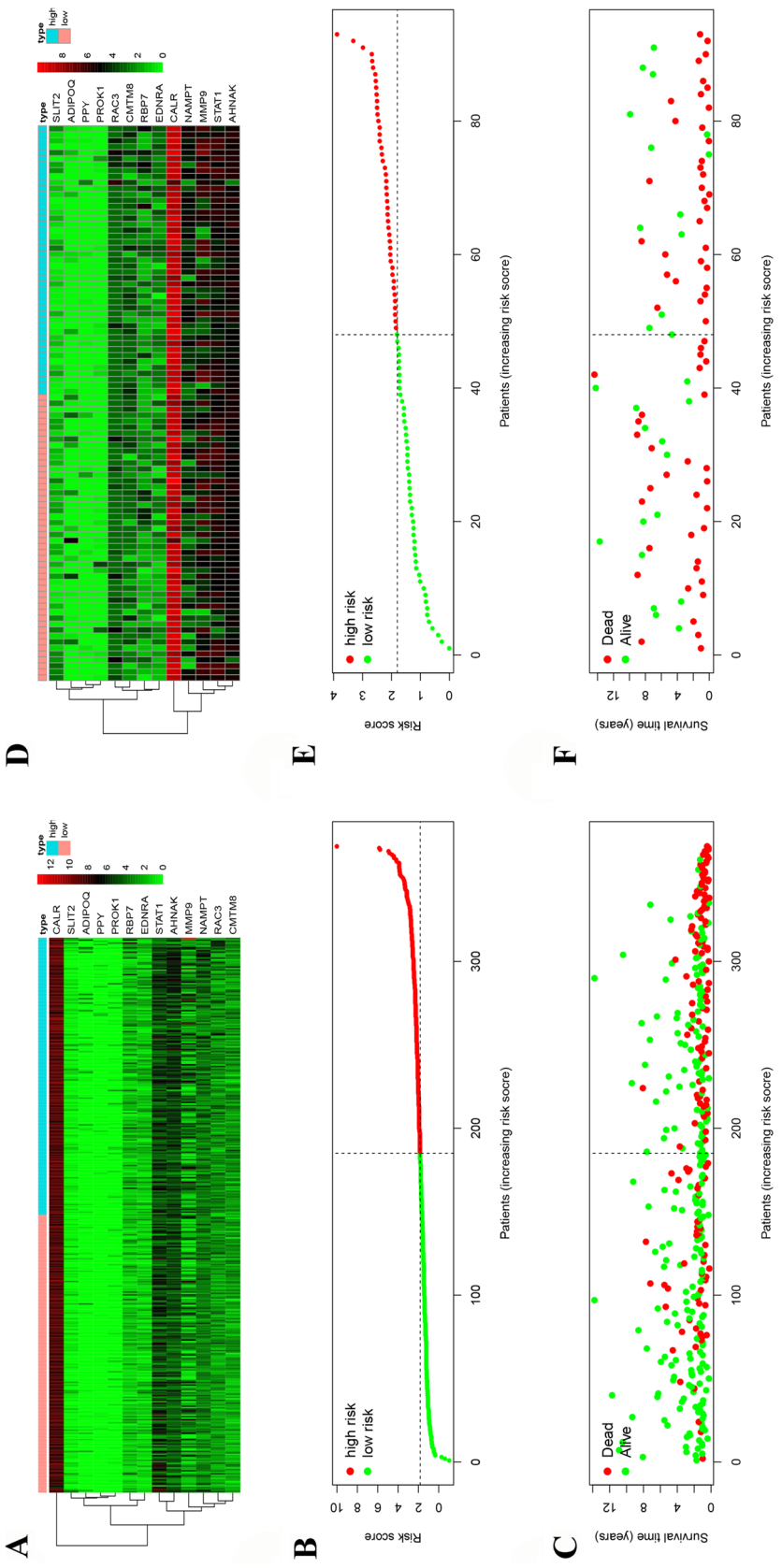

Figure 4. Development of the immune-related gene prognostic index (IRGPI) and validation model: (**A**) Heatmap of expression profiles of included genes in IRGPI. (**B**) Rank of prognostic index and distribution of groups in IRGPI. (**C**) Survival status of patients in different groups in IRGPI. (**D**) Heatmap of expression profiles of included genes in validation model. (**E**) Rank of prognostic index and distribution of groups in validation model. (**F**) Survival status of patients in different groups in validation model.

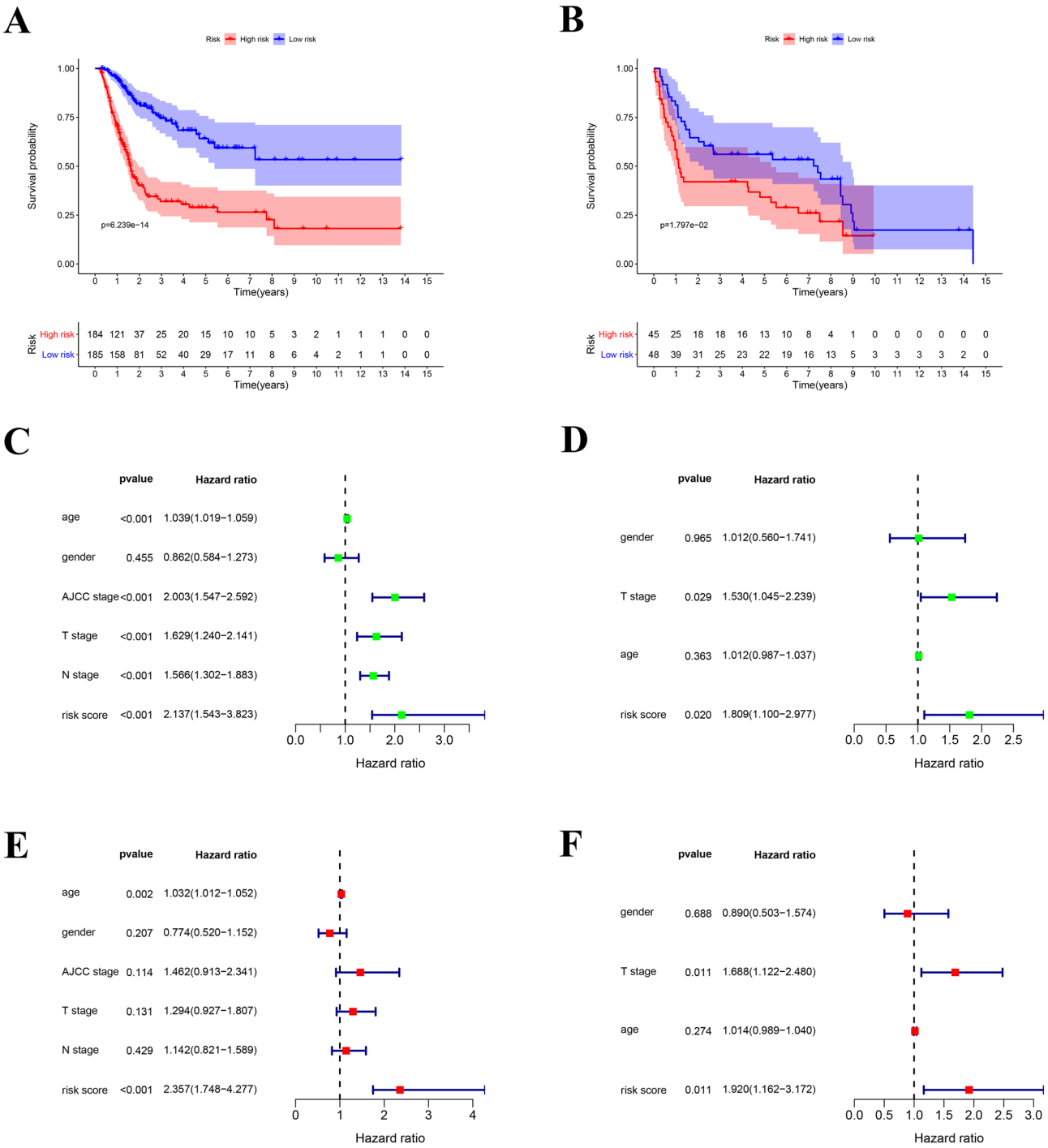

Figure 5. IRGPI and validation model for outcome prediction and relationship with clinical features: (**A**) patients in high-risk group suffered shorter overall survival in IRGPI. (**B**) The forest plot of univariate analyses of risk score with clinical features in IRGPI. (**C**) The forest plot of multivariate analyses of risk score with clinical features in IRGPI. (**D**) Patients in high-risk group suffered shorter overall survival in validation model. (**E**) The forest plot of univariate analyses of risk score with clinical features in validation model. (**F**) The forest plot of multivariate analyses of risk score with clinical features in validation model.

recent studies have demonstrated that M2-phenotype TAMs are the overwhelming immune cell type in the microenvironment of bladder cancer[43]. Thus, M2 macrophages can be used as a promising prognostic index and potential target for immunotherapy in bladder cancer.

We further investigated the potential mechanism of survival-associated IRGs and the clinical significance via analysis of the expression profiles of transcription factors. OGN, ELN, ANXA6, ILK and TGFB3 were identified as hub IRGs in the network. Osteoinductive factor (OGN) has been demonstrated to reduce cell proliferation and inhibit invasion in colorectal cancer[44]. A recent study reported that integrin-linked kinase (ILK) could promote

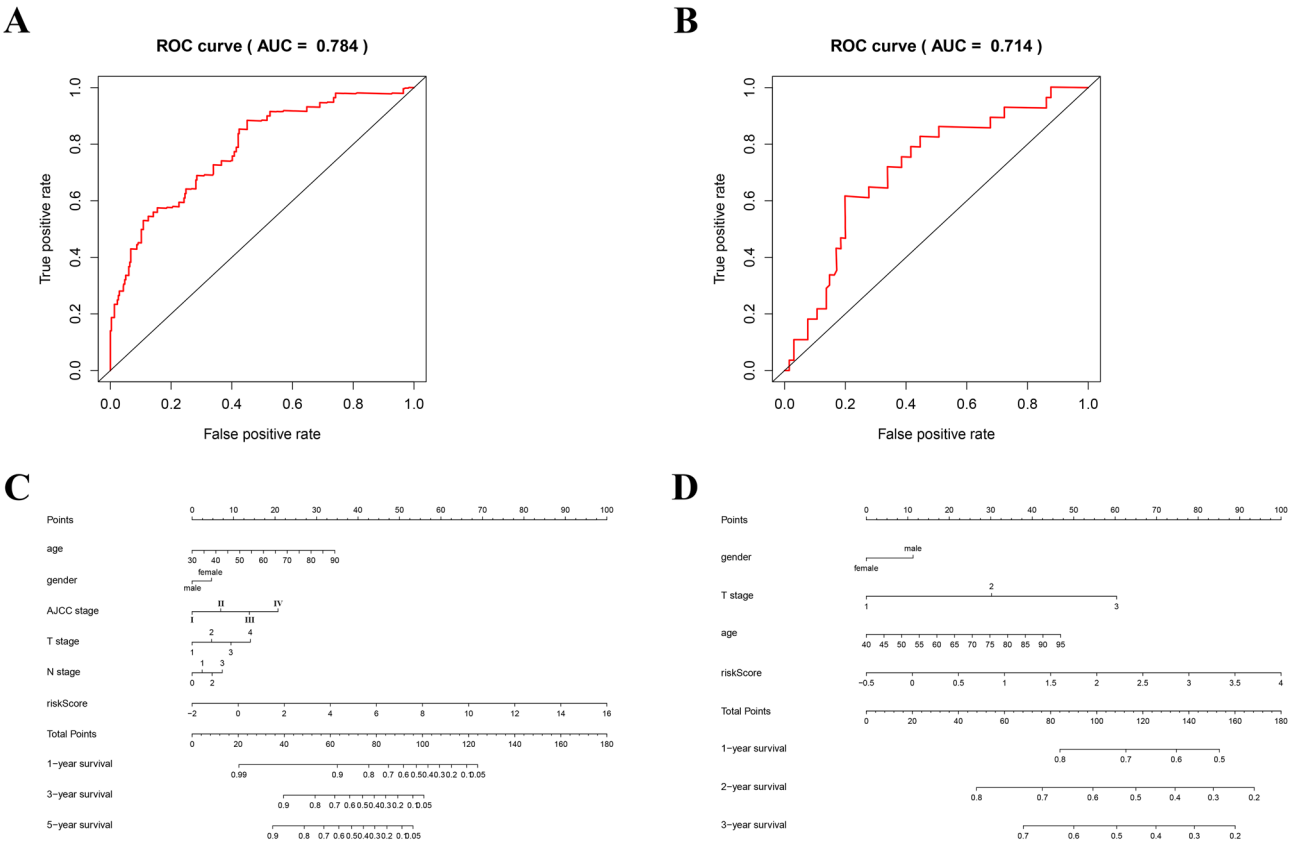

Figure 6. Verify the accuracy of IRGPI and validation model: (**A**) The ROC curve validation of prognostic value of IRGPI. (**B**) The ROC curve validation of prognostic value of validation model. (**C**) The nomogram of IRGPI. (**D**) The nomogram of validation model.

cell proliferation and migration in non-small-cell lung cancer[45]. Moreover, transforming growth factor (TGF)-B3 has been widely accepted as a crucial mediator of tumour progression[46–48]. MYH11, which encodes myosin heavy chain 11, a smooth muscle myosin protein, is closely associated with the composition of the fusion gene CBFB/MYH11 and participates in the initiation of acute myeloid leukaemia[49]. In general, previous studies have provided a limited understanding of the regulatory effects of IRGs on bladder cancer outcomes. The immunogenomic mechanisms of IRGs in bladder cancer are worthy of deep exploration.

Limitations

The present study still had several limitations. First, our prognostic index was based on gene expression data provided by TCGA, and the high price and long testing time might limit the application of our prognostic index in clinical practice. Second, because of limited clinical data, the present study failed to designate subgroups, and for patients receiving immunotherapy, our study might not accurately reflect the immune cell infiltration status. Moreover, the reliability of IRGs and their clinical prognostic value require further investigation for verification.

Conclusion

To the best of our knowledge, this is the first study to perform an immunogenomic landscape analysis and construct an IRG-related prognostic index in bladder cancer. In addition, our study revealed that macrophage infiltration was positively correlated with bladder cancer outcome, providing a more comprehensive understanding of the immune response in the tumour microenvironment and promising immunotherapeutic targets for clinical practice.

Methods

Data acquisition and processing. Transcriptome RNA-sequencing and clinical data from bladder cancer patients were obtained from the TCGA data portal (https://portal.gdc.cancer.gov/). A total of 411 bladder cancer tissues and 19 normal bladder tissues were included in the present study. The immune-related gene list was downloaded from the Immunology Database and Analysis Portal (ImmPort) database[50].

Identification of DEGs, DEIRGs and survival-associated IRGs. The differentially expressed genes (DEGs) were identified by using the edgeR package in the R language (https://bioconductor.org/packages/edgeR/) to further analyse the data. A |log2 fold change (FC)|> 2.0 and false discovery rate (FDR) adjusted to a P

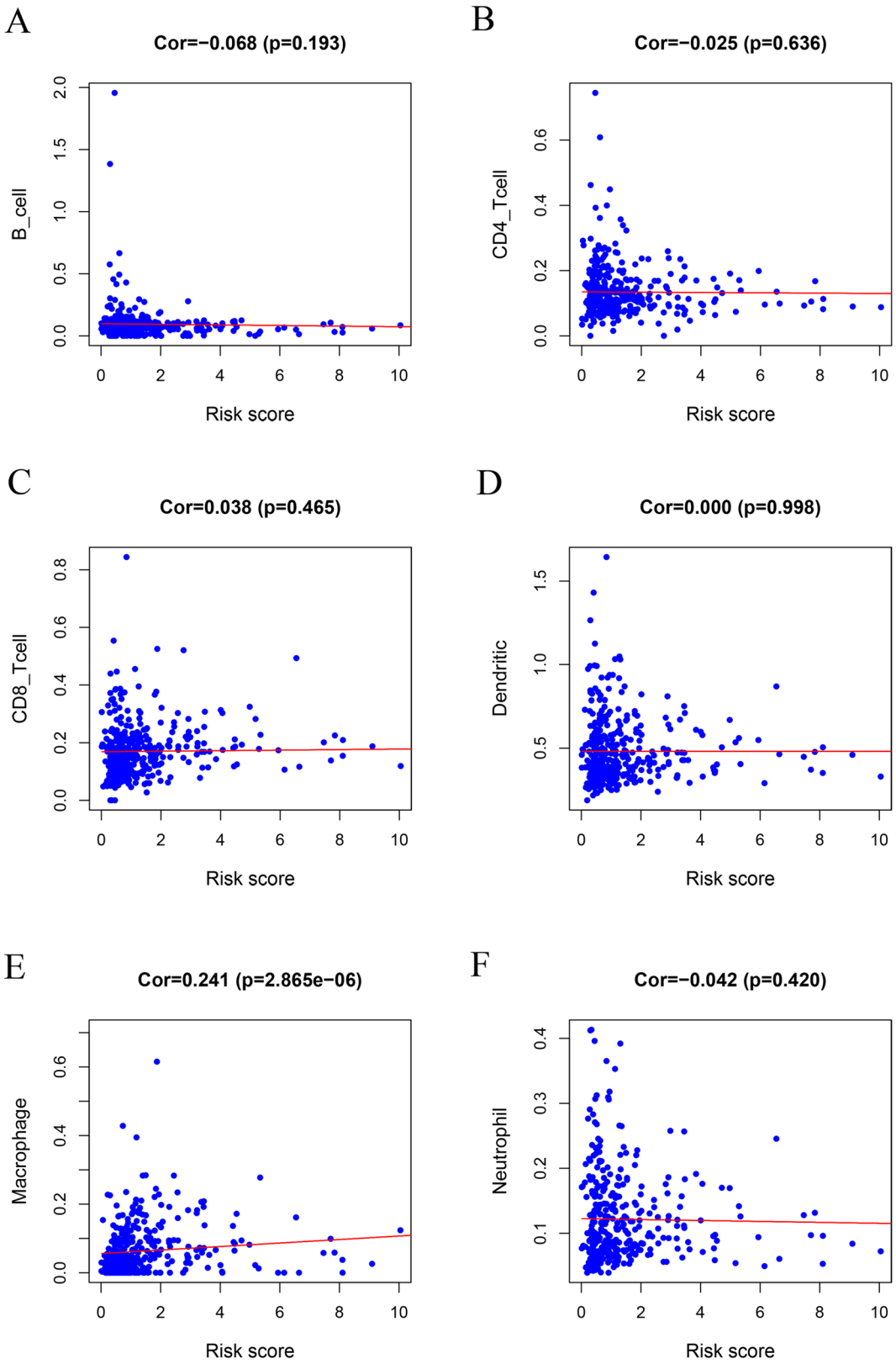

Figure 7. Relationships between the immune-related prognostic index and infiltration of six types of immune cells: (**A**) B cells; (**B**) CD4 T cells; (**C**) CD8 T cells; (**D**) dendritic cells; (**E**) macrophages; and (**F**) neutrophils.

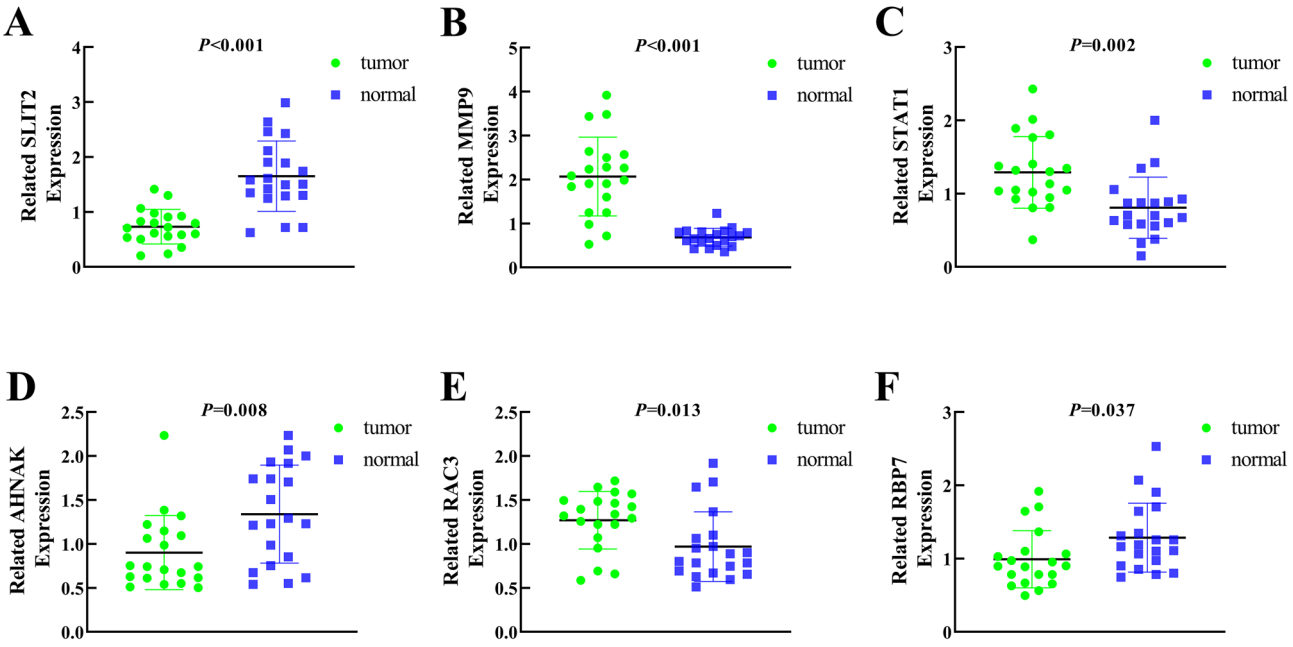

Figure 8. Related expression levels of relevant key genes. (**A**) SLIT2; (**B**) MMP9; (**C**) STAT1; (**D**) AHNAK; (**E**) RAC3; (**F**) RBP7.

value < 0.01 were set as the thresholds[51]. In addition, volcano maps and heat maps of the DEGs were produced by using the gplots and heatmap packages in the edgeR package. By compared the immune-related gene lists, we obtained the DEIRGs. Survival-associated IRGs were selected by univariate Cox analysis, which was conducted using the R software survival package.

Functional enrichment analysis. To understand the underlying biological mechanisms of the IRGs, GO annotation and KEGG pathway analyses were conducted by the DAVID (Database for Annotation, Visualization, and Integrated discovery; https://david.ncifcrf.gov/) online tool[52] and clusterProfiler, which is an R package for functional classification and enrichment of gene clusters using hypergeometric distribution. The GO plot package of the R software was used to display the results of the GO and KEGG analyses. GO and KEGG enrichment analyses were based on the threshold of $p < 0.01$.

Development of the immune-related gene prognostic index (IRGPI) and validation model. Prognostic risk score was obtained for all patients by univariate COX regression analysis and lasso-penalized Cox regression. Cox regression analysis was tested by Akaike Information Criterion (AIC) to identify the predictive model with the best explanatory and informative efficacy[53]. Patients were classified into high risk score group and low risk score group by median risk score. To further verify the feasibility of the prognostic model, we also divided GSE31684 patients into two groups according to the median risk score. The survival of the two groups of patients was analyzed by KM curve.

Relationship between IRGPI and immune cell infiltration. The TIMER online database analyses and visualizes the abundances of tumour-infiltrating immune cells[54]. TIMER was used to reanalyse gene expression data from TCGA, which included 10,897 samples across 32 cancer types, to estimate the abundance of six subtypes of tumour-infiltrating immune cells, including CD4 cells, CD8 cells, B cells, macrophages, dendritic cells and neutrophils. TIMER can be easily used to determine the relationship between immune cell infiltration and other parameters. We downloaded the immune infiltrate levels of bladder cancer patients and calculated associations between the IRGPI and immune cell infiltration.

Regulatory mechanisms of survival-associated IRGs. The Cistrome Cancer database is a resource for experimental and computational cancer biology research and contains a total of 318 transcription factors (TFs). To explore how TFs regulate the clinically relevant IRGs, we screened out clinically relevant TFs to construct the regulatory network of relevant IRGs and potential TFs.

Quantitative real-time PCR (qRT-PCR). Total RNA was obtained from 20 patients with breast cancer using TRIzol reagent (Invitrogen), and then reverse transcribed with the First Strand cDNA synthesis kit (New England Biolabs (Beijing) LTD., China). We performed amplifications with a SYBR Green PCR kit (Applied Biological Materials, Canada) according to the manufacturer's instructions on Applied Biosystems 7500Real-Time PCR System (Applied Biosystems, USA). The expression of RNA was normalized against GAPDH using the

2-ΔΔCt method. The PCR primers used are shown in Supplementary material 11. Three separate experiments were performed.

Statistical analysis. We performed survival analysis for patients with the prognostic model by using the "survival" package in R. Survival curves were generated using the Kaplan–Meier method and the log-rank test to compare the difference between the two groups. The AUC of the survival ROC curve was calculated via the survival ROC R software package to validate the performance of the prognostic signature[55]. p values of < 0.05 were considered statistically significant.

Received: 4 October 2019; Accepted: 17 June 2020
Published online: 12 November 2020

References

1. Siegel, R. L., Miller, K. D. & Jemal, A. Cancer statistics, 2018. *CA Cancer J. Clin.* **68**(1), 7–30 (2018).
2. Antoni, S. *et al.* Bladder cancer incidence and mortality: a global overview and recent trends. *Eur. Urol.* **71**(1), 96–108 (2017).
3. Barocas, D. A. *et al.* Surveillance and treatment of non-muscle-invasive bladder cancer in the USA. *Adv. Urol.* **2012**, 421709 (2012).
4. Garcia, J. A. & Dreicer, R. Systemic chemotherapy for advanced bladder cancer: update and controversies. *J. Clin. Oncol.* **24**(35), 5545–5551 (2006).
5. Sternberg, C. N. *et al.* Chemotherapy for bladder cancer: treatment guidelines for neoadjuvant chemotherapy, bladder preservation, adjuvant chemotherapy, and metastatic cancer. *Urology* **69**(1 Suppl), 62–79 (2007).
6. Senovilla, L. *et al.* Trial watch: prognostic and predictive value of the immune infiltrate in cancer. *Oncoimmunology* **1**(8), 1323–1343 (2012).
7. Coussens, L. M. & Werb, Z. Inflammation and cancer. *Nature* **420**(6917), 860–867 (2002).
8. Hagerling, C., Casbon, A. J. & Werb, Z. Balancing the innate immune system in tumor development. *Trends Cell Biol.* **25**(4), 214–220 (2015).
9. Powles, T. *et al.* MPDL3280A (anti-PD-L1) treatment leads to clinical activity in metastatic bladder cancer. *Nature* **515**(7528), 558–562 (2014).
10. Jia, H. *et al.* Immunotherapy for triple-negative breast cancer: existing challenges and exciting prospects. *Drug Resist. Updat.* **32**, 1–15 (2017).
11. Spigel, D. R. *et al.* Phase 1/2 study of the safety and tolerability of nivolumab plus crizotinib for the first-line treatment of anaplastic lymphoma kinase translocation: positive advanced non-small cell lung cancer (CheckMate 370). *J. Thorac. Oncol.* **13**(5), 682–688 (2018).
12. Vari, F. *et al.* Immune evasion via PD-1/PD-L1 on NK cells and monocyte/macrophages is more prominent in Hodgkin lymphoma than DLBCL. *Blood* **131**(16), 1809–1819 (2018).
13. Liotta, L. A. & Kohn, E. C. The microenvironment of the tumour-host interface. *Nature* **411**(6835), 375–379 (2001).
14. Gentles, A. J. *et al.* The prognostic landscape of genes and infiltrating immune cells across human cancers. *Nat. Med.* **21**(8), 938–945 (2015).
15. Jiang, B. *et al.* An immune-related gene signature predicts prognosis of gastric cancer. *Med. (Baltim.)* **98**(27), e16273 (2019).
16. Yang, W. *et al.* Immune signature profiling identified prognostic factors for gastric cancer. *Chin. J. Cancer Res.* **31**(3), 463–470 (2019).
17. D'angelo, A. *et al.* Tumour infiltrating lymphocytes and immune-related genes as predictors of outcome in pancreatic adenocarcinoma. *PLoS ONE* **14**(8), e0219566 (2019).
18. Lin, P. *et al.* Development of a prognostic index based on an immunogenomic landscape analysis of papillary thyroid cancer. *Aging (Albany NY)* **11**(2), 480–500 (2019).
19. Yu, Y. *et al.* Association of survival and immune-related biomarkers with immunotherapy in patients with non-small cell lung cancer: a meta-analysis and individual patient-level analysis. *JAMA Netw. Open* **2**(7), e196879 (2019).
20. Sahai, E. & Marshall, C. J. RHO-GTPases and cancer. *Nat. Rev. Cancer* **2**(2), 133–142 (2002).
21. Mira, J. P., Benard, V., Groffen, J., Sanders, L. C. & Knaus, U. G. Endogenous, hyperactive Rac3 controls proliferation of breast cancer cells by a p21-activated kinase-dependent pathway. *Proc. Natl. Acad. Sci. USA* **97**(1), 185–189 (2000).
22. Walker, M. P. *et al.* RAC3 is a pro-migratory co-activator of ERalpha. *Oncogene* **30**(17), 1984–1994 (2011).
23. Dong, S. *et al.* F-box protein complex FBXL19 regulates TGFbeta1-induced E-cadherin down-regulation by mediating Rac3 ubiquitination and degradation. *Mol. Cancer* **13**, 76 (2014).
24. Wang, G. *et al.* Rac3 regulates cell proliferation through cell cycle pathway and predicts prognosis in lung adenocarcinoma. *Tumour Biol.* **37**(9), 12597–12607 (2016).
25. Zhang, C. *et al.* Rac3 regulates cell invasion, migration and EMT in lung adenocarcinoma through p38 MAPK pathway. *J. Cancer* **8**(13), 2511–2522 (2017).
26. Kudryavtseva, A. V. *et al.* Bioinformatic identification of differentially expressed genes associated with prognosis of locally advanced lymph node-positive prostate cancer. *J. Bioinform. Comput. Biol.* **17**(1), 1950003 (2019).
27. Yu, J. C., Pickard, J. D. & Davenport, A. P. Endothelin ETA receptor expression in human cerebrovascular smooth muscle cells. *Br. J. Pharmacol.* **116**(5), 2441–2446 (1995).
28. Rachidi, S. M., Qin, T., Sun, S., Zheng, W. J. & Li, Z. Molecular profiling of multiple human cancers defines an inflammatory cancer-associated molecular pattern and uncovers KPNA2 as a uniform poor prognostic cancer marker. *PLoS ONE* **8**(3), e57911 (2013).
29. Laurberg, J. R. *et al.* High expression of GEM and EDNRA is associated with metastasis and poor outcome in patients with advanced bladder cancer. *BMC Cancer* **14**, 638 (2014).
30. Shankar, J. *et al.* Pseudopodial actin dynamics control epithelial-mesenchymal transition in metastatic cancer cells. *Cancer Res.* **70**(9), 3780–3790 (2010).
31. Chen, B. *et al.* AHNAK suppresses tumour proliferation and invasion by targeting multiple pathways in triple-negative breast cancer. *J. Exp. Clin. Cancer Res.* **36**(1), 65 (2017).
32. Zhao, Z. *et al.* AHNAK as a prognosis factor suppresses the tumor progression in glioma. *J. Cancer* **8**(15), 2924–2932 (2017).
33. Zhang, Z. *et al.* Upregulation of nucleoprotein AHNAK is associated with poor outcome of pancreatic ductal adenocarcinoma prognosis via mediating epithelial-mesenchymal transition. *J. Cancer* **10**(16), 3860–3870 (2019).
34. Dhanasekaran, D. N. & Johnson, G. L. MAPKs: function, regulation, role in cancer and therapeutic targeting. *Oncogene* **26**(22), 3097–3099 (2007).
35. Corteggio, A., Di Geronimo, O., Roperto, S., Roperto, F. & Borzacchiello, G. Activated platelet-derived growth factor beta receptor and Ras-mitogen-activated protein kinase pathway in natural bovine urinary bladder carcinomas. *Vet. J.* **191**(3), 393–395 (2012).

36. Zhao, L. *et al.* MAPK/AP-1 pathway regulates benzidine-induced cell proliferation through the control of cell cycle in human normal bladder epithelial cells. *Oncol. Lett.* **16**(4), 4628–4634 (2018).
37. Zhu, Q., Hong, B., Zhang, L. & Wang, J. Pyruvate kinase M2 inhibits the progression of bladder cancer by targeting MAKP pathway. *J. Cancer Res. Ther.* **14**(Supplement), S616–S621 (2018).
38. Chanmee, T., Ontong, P., Konno, K. & Itano, N. Tumor-associated macrophages as major players in the tumor microenvironment. *Cancers (Basel)* **6**(3), 1670–1690 (2014).
39. Laoui, D. *et al.* Tumor-associated macrophages in breast cancer: distinct subsets, distinct functions. *Int. J. Dev. Biol.* **55**(7–9), 861–867 (2011).
40. Tsutsui, S. *et al.* Macrophage infiltration and its prognostic implications in breast cancer: the relationship with VEGF expression and microvessel density. *Oncol. Rep.* **14**(2), 425–431 (2005).
41. Chen, J. J. *et al.* Up-regulation of tumor interleukin-8 expression by infiltrating macrophages: its correlation with tumor angiogenesis and patient survival in non-small cell lung cancer. *Clin. Cancer Res.* **9**(2), 729–737 (2003).
42. Wang, B. *et al.* High CD204+ tumor-infiltrating macrophage density predicts a poor prognosis in patients with urothelial cell carcinoma of the bladder. *Oncotarget* **6**(24), 20204–20214 (2015).
43. Xue, Y. *et al.* Tumorinfiltrating M2 macrophages driven by specific genomic alterations are associated with prognosis in bladder cancer. *Oncol. Rep.* **42**(2), 581–594 (2019).
44. Hu, X. *et al.* Osteoglycin (OGN) reverses epithelial to mesenchymal transition and invasiveness in colorectal cancer via EGFR/Akt pathway. *J. Exp. Clin. Cancer Res.* **37**(1), 41 (2018).
45. Karachaliou, N. *et al.* Integrin-linked kinase (ILK) and src homology 2 domain-containing phosphatase 2 (SHP2): novel targets in EGFR-mutation positive non-small cell lung cancer (NSCLC). *EBioMedicine* **39**, 207–214 (2019).
46. Vagenas, K., Spyropoulos, C., Gavala, V. & Tsamandas, A. C. TGFbeta1, TGFbeta2, and TGFbeta3 protein expression in gastric carcinomas: correlation with prognostics factors and patient survival. *J. Surg. Res.* **139**(2), 182–188 (2007).
47. Tang, M. R. *et al.* Prognostic significance of in situ and plasma levels of transforming growth factor beta1, -2 and -3 in cutaneous melanoma. *Mol. Med. Rep.* **11**(6), 4508–4512 (2015).
48. Ma, J. *et al.* Low transforming growth factor-beta3 expression predicts tumor malignancy in meningiomas. *World Neurosurg.* **125**, e353–e360 (2019).
49. Liu, P. *et al.* Fusion between transcription factor CBF beta/PEBP2 beta and a myosin heavy chain in acute myeloid leukemia. *Science* **261**(5124), 1041–1044 (1993).
50. Bhattacharya, S. *et al.* ImmPort: disseminating data to the public for the future of immunology. *Immunol. Res.* **58**(2–3), 234–239 (2014).
51. Robinson, M. D., Mccarthy, D. J. & Smyth, G. K. edgeR: a Bioconductor package for differential expression analysis of digital gene expression data. *Bioinformatics* **26**(1), 139–140 (2010).
52. Dennis, G. Jr. *et al.* DAVID: database for annotation, visualization, and integrated discovery. *Genome Biol.* **4**(5), P3 (2003).
53. Akaike, H. A new look at the statistical model identification. *IEEE Trans. Autom. Control* **19**(6), 716–723. https://doi.org/10.1109/TAC.1974.1100705 (1974).
54. Li, T. *et al.* TIMER: a web server for comprehensive analysis of tumor-infiltrating immune cells. *Cancer Res.* **77**(21), e108–e110 (2017).
55. Heagerty, P. J., Lumley, T. & Pepe, M. S. Time-dependent ROC curves for censored survival data and a diagnostic marker. *Biometrics* **56**(2), 337–344 (2000).

Acknowledgements

The authors express sincere gratitude to the ImmPort, TIMER and TCGA databases for the availability of data.

Author contributions

Y.Q.H. and W.J.W. contributed conception and design of the study; J.Z., H.W. and T.M. organized the database; Y.H. and M.S. performed the statistical analysis; W.S. and J.J.W. wrote the first draft of the manuscript; J.P.S., M.Y.W. and C.L. wrote sections of the manuscript. All authors contributed to manuscript revision, read and approved the submitted version.

Funding

The authors disclosed receipt of the following financial support for the research, authorship, and/or publication of this article: this work was supported by the Science and Education for Health Foundation of Suzhou for Youth (Grant Nos. kjxw2018030 and kjxw2018032), the Science and Technology Project Foundation of Suzhou (Grant No. SS201651), the medical key discipline foundation of Jiangsu Province (Grant No. ZDXKC2016007) and the Education Research Project Foundation of Nanjing Medical University (Grant No. FZS-ZD-201701).

Competing interests

The authors declare no competing interests.

Additional information

Supplementary information is available for this paper at https://doi.org/10.1038/s41598-020-76688-w.

Correspondence and requests for materials should be addressed to W.-J.W.

Reprints and permissions information is available at www.nature.com/reprints.

Publisher's note Springer Nature remains neutral with regard to jurisdictional claims in published maps and institutional affiliations.